On Operator Filtering for Integral Equations: The High-Order Case

On Operator Filtering for Integral Equations: the High-Order Case

Johann Bourhis[(1)], Damiano Franzò[(1)], Clément Henry[(2)], Adrien Merlini[(2)], and Francesco P. Andriulli[(1)]

[(1)] Politecnico di Torino, Turin, Italy
[(2)] IMT Atlantique, Brest, France

***Abstract*—In this work, we extend the standard quasi-Helmholtz filters to high-order discretizations in the context of the boundary element method. This generalization allows preconditioning integral equations such as the electric field integral equation (EFIE) in the h-refinement regime while preserving the accuracy gain of high-order discretizations. The theoretical framework will be corroborated by numerical results that validate the effectiveness of the proposed strategy when stabilizing the refinement-dependent spectral behavior of the high-order discretized EFIE.**

I. Introduction

Solving the electric field integral equation (EFIE) via the boundary element method yields highly accurate solutions when leveraging high-order discretizations [1]. Unfortunately, the EFIE suffers from severe ill-conditioning at low frequencies and for densely discretized geometries, which causes a loss of accuracy and a higher number of iterations in the solution process. An effective approach to treat the low-frequency breakdown is to rely on the quasi-Helmholtz projectors, that have been recently generalized to the high-order framework [2]. However, the projector-based EFIE remains ill-conditioned for high mesh density (referred to as h-refinement breakdown), and additional strategies are therefore required to remedy both ill-conditioning problems at the same time.

To this aim, the quasi-Helmholtz Laplacian filters, recently introduced in [3], constitute an efficient method to tackle simultaneously the low-frequency and the h-refinement breakdowns without the requirement of barycentric refinements. One may consider such filtered projectors as an extension of the quasi-Helmholtz projectors that offers the additional possibility of flattening the EFIE spectrum [3], yielding a well-conditioned formulation from medium to low-frequency and for arbitrary mesh density. Leveraging previous contributions [2], [3], this paper generalizes the quasi-Helmholtz Laplacian filters to high-order discretizations. The effectiveness of the newly introduced filters will be illustrated in the stabilization of the EFIE in the h-refinement and low frequency regimes.

II. Background and notations

We consider a closed and simply connected surface boundary Γ modeling a perfectly electrically conducting (PEC) object with outward pointing normal $\widehat{\boldsymbol{n}}$ and approximated by a mesh of curvilinear triangular cells. We denote by $\widehat{\boldsymbol{r}} = (u, v)^T$ the coordinates in the reference triangle $\widehat{K}$. For each cell K of the mesh, we define a local-to-global mapping $\boldsymbol{r} := F_K(\widehat{\boldsymbol{r}})$, with associated Jacobian $\mathbf{J}_{F_K} = (\partial_u F_K, \partial_v F_K)^T$ and elementary surface area $\mathcal{J}_K = |\partial_u F_K \times \partial_v F_K|$.

We denote by $\mathbb{P}_r(\widehat{K})$ the space of scalar polynomials of degree up to order r on $\widehat{K}$. The Raviart-Thomas space $\mathbb{RT}_r$ contains functions $\boldsymbol{\psi}(\boldsymbol{r}) = \pm\frac{1}{\mathcal{J}_K}\mathbf{J}_{F_K}^T\widehat{\boldsymbol{\psi}}(\widehat{\boldsymbol{r}})$ having edge normal continuity, where $\widehat{\boldsymbol{\psi}} \in \mathbb{P}_r^2(\widehat{K}) + \widehat{\boldsymbol{r}}\mathbb{P}_r(\widehat{K})$. The continuous Galerkin space $\mathbb{CG}_{r+1}$ contains functions $\lambda(\boldsymbol{r}) = \widehat{\lambda}(\widehat{\boldsymbol{r}})$ having edge continuity, where $\widehat{\lambda} \in \mathbb{P}_{r+1}(\widehat{K})$. The discontinuous Galerkin space $\mathbb{DG}_r$ contains functions $\sigma(\boldsymbol{r}) = \frac{1}{\mathcal{J}_K}\widehat{\sigma}(\widehat{\boldsymbol{r}})$ where $\widehat{\sigma} \in \mathbb{P}_r(\widehat{K})$. In the following, we consider interpolatory bases of these finite element spaces. We respectively denote by $\{\lambda_l\}_{l=1}^L$ the continuous Lagrange basis of $\mathbb{CG}_{r+1}$, by $\{\boldsymbol{\psi}_n\}_{n=1}^N$ the Graglia-Wilton-Peterson [1] (GWP) basis of $\mathbb{RT}_r$, and by $\{\sigma_s\}_{s=1}^S$ the discontinuous Lagrange basis of $\mathbb{DG}_r$. In absence of handles, apertures, and junctions, and denoting by E, V, and C the number of edges, vertices, and cells of the mesh, $L = r(r-1)C/2 + rE + V$, $N = r(r+1)C + (r+1)E$, $S = (r+1)(r+2)C/2$ and $N = (L-1) + (S-1)$ [2].

Solving the EFIE yields the surface current density $\boldsymbol{J}$ induced by a time-harmonic incident field $\boldsymbol{E}^{\text{inc}}$. The equation reads $\left(jk\,\mathcal{T}_s + \frac{1}{jk}\,\mathcal{T}_h\right)\boldsymbol{J} = -\widehat{\boldsymbol{n}} \times \frac{1}{\eta}\boldsymbol{E}^{\text{inc}}$, where k is the wavenumber, η is the characteristic impedance, $(\mathcal{T}_s\boldsymbol{J})(\boldsymbol{r}) = \widehat{\boldsymbol{n}}(\boldsymbol{r}) \times \int_\Gamma \frac{e^{-jk|\boldsymbol{r}-\boldsymbol{r}'|}}{4\pi|\boldsymbol{r}-\boldsymbol{r}'|}\boldsymbol{J}(\boldsymbol{r}')\,\mathrm{d}S(\boldsymbol{r}')$ and $(\mathcal{T}_h\boldsymbol{J})(\boldsymbol{r}) = -\widehat{\boldsymbol{n}} \times \boldsymbol{\nabla}_\Gamma \int_\Gamma \frac{e^{-jk|\boldsymbol{r}-\boldsymbol{r}'|}}{4\pi\|\boldsymbol{r}-\boldsymbol{r}'\|}\boldsymbol{\nabla}'_\Gamma \cdot \boldsymbol{J}(\boldsymbol{r}')\,\mathrm{d}S(\boldsymbol{r}')$ are the vector and scalar potentials, respectively, and $\boldsymbol{\nabla}_\Gamma$ is the surface nabla operator. The current is approximated by a linear combination of GWP functions $\boldsymbol{J}(\boldsymbol{r}) \approx \sum_{n=1}^N \left[\boldsymbol{j}\right]_n \boldsymbol{\psi}_n(\boldsymbol{r})$, and the equation is tested by rotated functions $\{\widehat{\boldsymbol{n}} \times \boldsymbol{\psi}\}_{n=1}^N$ which yield a system matrix in the form $\mathbf{T}\boldsymbol{j} = \boldsymbol{e}$ with $\mathbf{T} = jk\,\mathbf{T}_s + \frac{1}{jk}\,\mathbf{T}_h$ (refer to [2] for definitions). This system suffers from low-frequency and dense mesh discretization breakdowns. More precisely, its ill-conditioning behavior is expressed as $\mathrm{cond}\,(\mathbf{T}) \lesssim O(1/(kh)^2)$, with $h \to 0$ and $k \to 0$, where h is the average cell diameter of the mesh [3].

In the following, we denote the Gram matrix associated with two sets of (scalar or vector) functions $\{\boldsymbol{f}_i\}_{i=1}^I$ and $\{\boldsymbol{g}_j\}_{j=1}^J$ by $\mathbf{G}_{\boldsymbol{f},\boldsymbol{g}} \in \mathbb{R}^{I\times J}$, where $[\mathbf{G}_{\boldsymbol{f},\boldsymbol{g}}]_{ij} = \int_\Gamma \boldsymbol{f}_i(\boldsymbol{r}) \cdot \boldsymbol{g}_j(\boldsymbol{r})\,\mathrm{d}S(\boldsymbol{r})$.

III. High-order quasi-Helmholtz projectors

The expansion coefficients $\boldsymbol{j}$ can be decomposed in the form $\boldsymbol{j} = \boldsymbol{\Lambda}\boldsymbol{l} + \boldsymbol{\Sigma}\boldsymbol{s}$, where $\boldsymbol{\Lambda}$ and $\boldsymbol{\Sigma}$ are respectively the GWP-to-Loop and GWP-to-Star transform matrices, defined as [2]

$$\boldsymbol{\Lambda} = \mathbf{G}_{\boldsymbol{\psi},\boldsymbol{\psi}}^{-1}\mathbf{G}_{\boldsymbol{\psi},\widehat{\boldsymbol{n}}\times\boldsymbol{\nabla}_\Gamma\lambda} \quad \text{and} \quad \boldsymbol{\Sigma} = \mathbf{G}_{\boldsymbol{\nabla}_\Gamma\cdot\boldsymbol{\psi},\sigma}\,, \tag{1}$$

DOI: 10.1109/AP-S/INC-USNC-URSI52054.2024.10686349

which also guarantees the orthogonality properties $\mathbf{\Sigma}^T\mathbf{\Lambda}=\mathbf{0}$, $\mathbf{\Lambda}^T\mathbf{T}_h=\mathbf{0}$ and $\mathbf{T}_h\mathbf{\Lambda}=\mathbf{0}$ [2]. From this decomposition, we build the general form of the projectors on the Loop and the Star subspaces, respectively $\mathbf{P}^{\mathbf{\Lambda}}=\mathbf{\Lambda}(\mathbf{\Lambda}^T\mathbf{\Lambda})^+\mathbf{\Lambda}^T$ and $\mathbf{P}^{\mathbf{\Sigma}}=\mathbf{\Sigma}(\mathbf{\Sigma}^T\mathbf{\Sigma})^+\mathbf{\Sigma}^T$, where $+$ denotes the Moore-Penrose pseudoinverse. These projectors are orthogonal to each other, i.e., $\mathbf{P}^{\mathbf{\Lambda}}\mathbf{P}^{\mathbf{\Sigma}}=\mathbf{0}$.

IV. High-order quasi-Helmholtz Laplacian filters

In order to analyze the proposed strategy, we normalize the EFIE leveraging inverse square roots of Gram matrices. The normalized EFIE reads

$$\widetilde{\mathbf{T}}\widetilde{\boldsymbol{j}}=\widetilde{\boldsymbol{e}} \quad \text{with} \quad \widetilde{\mathbf{T}}=jk\,\widetilde{\mathbf{T}}_s+\frac{1}{jk}\,\widetilde{\mathbf{T}}_h \tag{2}$$

where $\widetilde{\mathbf{T}}_s=\mathbf{G}_{\psi,\psi}^{-1/2}\mathbf{T}_s\mathbf{G}_{\psi,\psi}^{-1/2}$, $\widetilde{\mathbf{T}}_h=\mathbf{G}_{\psi,\psi}^{-1/2}\mathbf{T}_h\mathbf{G}_{\psi,\psi}^{-1/2}$, $\widetilde{\boldsymbol{e}}=\mathbf{G}_{\psi,\psi}^{-1/2}\boldsymbol{e}$ and $\widetilde{\boldsymbol{j}}=\mathbf{G}_{\psi,\psi}^{1/2}\boldsymbol{j}$. The normalized Loop and Star transform matrices are $\widetilde{\mathbf{\Lambda}}=\mathbf{G}_{\psi,\psi}^{1/2}\mathbf{\Lambda}\mathbf{G}_{\lambda,\lambda}^{-1/2}$ and $\widetilde{\mathbf{\Sigma}}=\mathbf{G}_{\psi,\psi}^{-1/2}\mathbf{\Sigma}\mathbf{G}_{\sigma,\sigma}^{-1/2}$. One can check that the orthogonality properties analog to the ones obtained with the non-normalized Loops and Stars still hold. We can subsequently build the normalized quasi-Helmholtz projectors as

$$\mathbf{P}^{\widetilde{\mathbf{\Lambda}}}=\widetilde{\mathbf{\Lambda}}(\widetilde{\mathbf{\Lambda}}^T\widetilde{\mathbf{\Lambda}})^+\widetilde{\mathbf{\Lambda}}^T \quad \text{and} \quad \mathbf{P}^{\widetilde{\mathbf{\Sigma}}}=\widetilde{\mathbf{\Sigma}}(\widetilde{\mathbf{\Sigma}}^T\widetilde{\mathbf{\Sigma}})^+\widetilde{\mathbf{\Sigma}}^T\,. \tag{3}$$

Note that the matrices that we need to pseudoinvert in (3) are Galerkin approximations of the Laplace eigenvalue problem: based on the standard discretization using $\mathbb{CG}_{r+1}$ functions

$$\widetilde{\mathbf{\Lambda}}^T\widetilde{\mathbf{\Lambda}}=\mathbf{G}_{\lambda,\lambda}^{-1/2}\mathbf{G}_{\boldsymbol{\nabla}_\Gamma\lambda,\boldsymbol{\nabla}_\Gamma\lambda}\mathbf{G}_{\lambda,\lambda}^{-1/2}\,, \tag{4}$$

and based on the mixed-form discretization using $\mathbb{RT}_r$–$\mathbb{DG}_r$ functions [4]

$$\widetilde{\mathbf{\Sigma}}^T\widetilde{\mathbf{\Sigma}}=\mathbf{G}_{\sigma,\sigma}^{-1/2}\mathbf{G}_{\sigma,\boldsymbol{\nabla}_\Gamma\cdot\psi}\mathbf{G}_{\psi,\psi}^{-1}\mathbf{G}_{\boldsymbol{\nabla}_\Gamma\cdot\psi,\sigma}\mathbf{G}_{\sigma,\sigma}^{-1/2}\,. \tag{5}$$

Additionally, for Lipschitz boundaries, the eigenvalues of both discrete operators converge to the continuous Laplacian eigenvalues with rate $h^{2(r+1)}$ [4]. As it concerns the continuous Laplacian eigenvalues, they are known to increase linearly with their index, which is one of the main results that enable an effective rescaling of the filtered Laplacian operators [3].

We now define the filtered quasi-Helmholtz projectors as $\mathbf{P}_n^{\mathbf{A}}=\mathbf{A}(\mathbf{A}^T\mathbf{A})_n^+\mathbf{A}^T$, where $\mathbf{A}$ stands for either $\widetilde{\mathbf{\Lambda}}$ or $\widetilde{\mathbf{\Sigma}}$, while $(\mathbf{A}^T\mathbf{A})_n$ is the eigenvalue decomposition of $\mathbf{A}^T\mathbf{A}$ truncated after its first n smallest eigenvalues [3]. Next, we define the wavelet-like projectors on the range of $\mathbf{A}$

$$\begin{aligned}\mathbf{W}_\ell^{\mathbf{A}}&=\mathbf{P}_{2^\ell-1}^{\mathbf{A}}-\mathbf{P}_{2^{\ell-1}-1}^{\mathbf{A}}\,,\quad \ell=2,\dots,\lfloor\log_2(N_A)\rfloor\\ \mathbf{W}_1^{\mathbf{A}}&=\mathbf{P}_1^{\mathbf{A}}\;;\;\mathbf{W}_{\lfloor\log_2(N_A)\rfloor+1}^{\mathbf{A}}=\mathbf{P}^{\mathbf{A}}-\mathbf{P}_{2^{\lfloor\log_2(N_A)\rfloor}-1}^{\mathbf{A}}\,.\end{aligned} \tag{6}$$

which allow defining the quasi-Helmholtz Laplacian filters

$$\mathbf{Q}^{\widetilde{\mathbf{\Lambda}}}=\sum_{\ell=1}^{\lfloor\log_2(L)\rfloor+1}\beta_\ell^{\widetilde{\mathbf{\Lambda}}}\,\mathbf{W}_\ell^{\widetilde{\mathbf{\Lambda}}} \quad \text{and} \quad \mathbf{Q}^{\widetilde{\mathbf{\Sigma}}}=\sum_{\ell=1}^{\lfloor\log_2(S)\rfloor+1}\beta_\ell^{\widetilde{\mathbf{\Sigma}}}\,\mathbf{W}_\ell^{\widetilde{\mathbf{\Sigma}}}\,, \tag{7}$$

with

$$\begin{aligned}\beta_\ell^{\widetilde{\mathbf{\Lambda}}}&=\|\mathbf{W}_\ell^{\widetilde{\mathbf{\Lambda}}}\widetilde{\mathbf{T}}_s\mathbf{W}_\ell^{\widetilde{\mathbf{\Lambda}}}\|^{-1/2}\,,\quad \ell=1,\dots,\lfloor\log_2(L)\rfloor+1,\\ \beta_\ell^{\widetilde{\mathbf{\Sigma}}}&=\|\mathbf{W}_\ell^{\widetilde{\mathbf{\Sigma}}}\widetilde{\mathbf{T}}_h\mathbf{W}_\ell^{\widetilde{\mathbf{\Sigma}}}\|^{-1/2}\,,\quad \ell=1,\dots,\lfloor\log_2(S)\rfloor+1\,.\end{aligned} \tag{8}$$

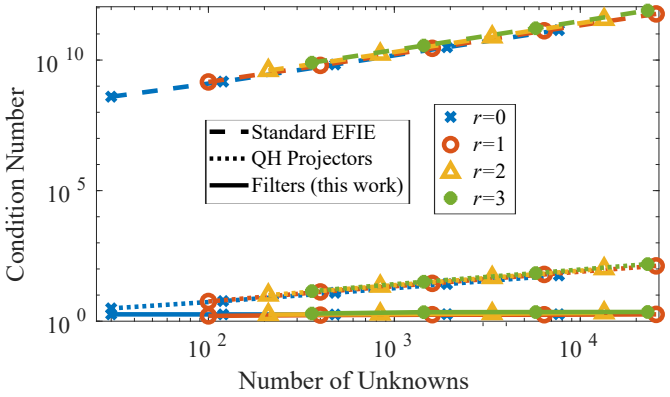

Fig. 1. Condition number of the system matrices as a function of the number of unknowns at a frequency of 10 kHz.

The preconditioning matrix is finally given by

$$\mathbf{Q}=k^{-1/2}\alpha^{\widetilde{\mathbf{\Lambda}}}\,\mathbf{Q}^{\widetilde{\mathbf{\Lambda}}}+jk^{1/2}\alpha^{\widetilde{\mathbf{\Sigma}}}\,\mathbf{Q}^{\widetilde{\mathbf{\Sigma}}}\,, \tag{9}$$

with

$$\alpha^{\widetilde{\mathbf{\Lambda}}}=\|\mathbf{Q}^{\widetilde{\mathbf{\Lambda}}}\widetilde{\mathbf{T}}_s\mathbf{Q}^{\widetilde{\mathbf{\Lambda}}}\|^{-1/2} \text{ and } \alpha^{\widetilde{\mathbf{\Sigma}}}=\|\mathbf{Q}^{\widetilde{\mathbf{\Sigma}}}\widetilde{\mathbf{T}}_h\mathbf{Q}^{\widetilde{\mathbf{\Sigma}}}\|^{-1/2}, \tag{10}$$

which yields the preconditioned system

$$\mathbf{Q}\widetilde{\mathbf{T}}\mathbf{Q}\boldsymbol{y}=\mathbf{Q}\widetilde{\boldsymbol{e}}\,, \tag{11}$$

with $\boldsymbol{j}=\mathbf{G}_{\psi,\psi}^{-1/2}\mathbf{Q}\boldsymbol{y}$.

V. Numerical validation

We compare the condition number of the quasi-Helmholtz Laplacian filters EFIE (11) along with the quasi-Helmholtz projectors EFIE (3)–[2] and the standard EFIE (2) (with normalization) for an increasingly dense mesh discretization of the unit sphere. The proposed technique provides bounded condition numbers, while the other formulations display condition numbers growing with the number of unknowns. Implementation details and additional validation results will be provided during the conference presentation.

Acknowledgment

The work of this paper has received funding from the EU H2020 research and innovation programme under the Marie Skłodowska-Curie grant agreement n° 955476 (project COMPETE), and from the European Innovation Council (EIC) through the European Union's Horizon Europe research Programme under Grant 101046748 (Project CEREBRO).

References

[1] R. Graglia, D. Wilton, and A. Peterson, "Higher order interpolatory vector bases for computational electromagnetics," *IEEE Transactions on Antennas and Propagation*, vol. 45, no. 3, pp. 329–342, 1997.

[2] J. Bourhis, A. Merlini, and F. P. Andriulli, "High-Order Quasi-Helmholtz Projectors: Definition, Analyses, Algorithms," *IEEE Transactions on Antennas and Propagation*, vol. 72, no. 4, pp. 3572–3579, 2024.

[3] A. Merlini, C. Henry, D. Consoli, L. Rahmouni, A. Dély, and F. P. Andriulli, "Laplacian Filtered Loop-Star Decompositions and Quasi-Helmholtz Filters: Definitions, Analysis, and Efficient Algorithms," *IEEE Transactions on Antennas and Propagation*, vol. 71, no. 12, pp. 9289–9302, 2023.

[4] B. Mercier, J. Osborn, J. Rappaz, and P. A. Raviart, "Eigenvalue approximation by mixed and hybrid methods," *Mathematics of Computation*, vol. 36, no. 154, pp. 427–453, 1981.